7 Structure of the Anaphylatoxins C3a and C5a

Dimitrios Morikis, M. Claire H. Holland, and John D. Lambris

CONTENTS

I. INTRODUCTION

The proinflammatory activities of the complement system are mostly mediated by the anaphylatoxins, C3a, C4a, and C5a. These compounds are small cationic peptides (approximately 10 kD in size) that are cleaved off the amino terminus of the α-chains of complement components 3 (C3), 4 (C4), and 5 (C5), respectively, upon complement activation. It has recently been shown that they can also be generated

independently of the three complement activation pathways, via the proteolytic activities of nonspecific enzymes.[1] The name anaphylatoxins arose in the early twentieth century in an effort to describe the activity present in complement-activated serum that was responsible for producing rapid death when injected into laboratory animals.[2] The isolation of the anaphylatoxins from complement-activated serum, and in more recent years, their production via recombinant technology, has led to a better refinement of their individual functional activities as well as their structural characteristics.

A. Functions of C3a and C5a

Most of our knowledge of the functional and structural activities of the anaphylatoxins comes from studies with C3a and C5a.[3,4] So far, C4a has received little attention, and this lack of interest may be due to the overall low activity of the peptide and the fact that no specific C4a receptor has yet been identified. The actions of C3a and C5a are mostly mediated via the C3a receptor (C3aR) and C5a receptor (C5aR or CD88), respectively.[3,4] Both are G-protein–coupled receptors present on myeloid and various nonmyeloid cells. Recently, a third type of receptor has been identified, termed C5L2, that appears to be uncoupled from G-protein signaling pathways and may serve as a decoy receptor for C5a rather than a functional receptor.[5,6] C3a and C5a bind to their respective receptors with nanomolar affinity and, depending on cell type and dose, exert multiple effects. The most notable of these effects is their ability to: (a) induce leukocyte chemotaxis, (b) release granule-associated enzymes and vasoactive mediators from granulocytes and mast cells, (c) activate NADPH oxidase in granulocytes, (d) increase vascular permeability and adhesion, (e) induce smooth muscle contractions, and (f) stimulate the release of specific cytokines by myeloid as well as various nonmyeloid cell types, such as endothelial and epithelial cells and astrocytes.[3,4]

The role of C3a in mediating proinflammatory responses is believed to be much more restricted than that of C5a. In addition, C3a is at least tenfold less active in inducing these responses compared to C5a.[4] Over the past years, it has become clear that the functions of C3a and C5a extend well beyond typical inflammatory-type responses.[7] Both C3a and C5a have been shown to play critical roles in complex developmental and morphogenetic processes, such as hematopoiesis, reproduction, liver regeneration, apoptosis, and central nervous system development.[8–12] The C3aR and C5aR are distributed widely in terms of both cell and tissue type, and the list of functions for C3a and C5a is still expected to expand.

Due to their potent inflammatory activities, the levels of C3a and C5a are tightly regulated by circulating carboxypeptidases, which cleave off the carboxy-terminal arginine residue of the molecules resulting in the formation of the desarginated peptides desArg-C3a and desArg-C5a, respectively.[3,13] Because the carboxy-terminus of both molecules is critical for functional activity, the desarginated peptides are generally significantly less active than the intact peptides. The only exception appears to be related to the lipogenic activity of C3a and desArg-C3a, which are equally active in this context.[14,15] Regulation of C3a and C5a activities have also been shown to occur at the cellular level, where excessive stimulation with either

peptide results in rapid homologous receptor desensitization and internalization.[16,17] Despite these regulatory mechanisms, various pathological conditions have been associated with acute and/or excessive production of C3a and/or C5a. Some of these pathologies include adult respiratory distress syndrome,[18] asthma,[19] septic shock,[20] rheumatoid arthritis,[21,22] inflammatory bowel disease,[23] Alzheimer's disease,[24] psoriasis,[25] and experimental bullous pemphigoid.[26] The development of several selective C5aR and C3aR antagonists has led to a better understanding of the involvement of the anaphylatoxins in the pathogenesis of these diseases, and may imply a potential therapeutic role for these small peptidic and nonpeptidic compounds.[22,27–31]

B. Sequence Alignments of C3a, C4a, and C5a

The anaphylatoxins are derived from three complement components that are genetically and structurally related, and it is therefore not surprising that also C3a, C4a, and C5a share sequence and structural similarities. Human C3a, C4a, and C5a have sequences of 77, 77, and 74 residues, respectively. Multiple alignment of the amino acid sequences of the three anaphylatoxins shows that 15 residues (19%) have been totally conserved between C3a, C4a, and C5a, six of which are the immutable disulfide bond forming cysteine residues (Figure 7.1). Individual comparisons show a 29% identity between C3a and C4a, 32% between C3a and C5a, and 36% between C3a and C4a. Of the human anaphylatoxins, only C5a is glycosylated at residue 64 (Asn). Although the presence of this oligosaccharide unit does not appear to affect the functional activity of C5a, its removal from the less potent desArg-C5a derivative resulted in enhanced leukocyte chemotaxis and C5aR binding, suggesting that glycosylation has a negative effect on the activity of this compound.[32] The anaphylatoxins share certain remarkable physical characteristics, such as their highly cationic nature and ability to withstand high temperatures and pH extremes without loss of activity.[33] The structures of C3a, C5a, and their desarginated derivatives have been

FIGURE 7.1 Alignment of amino acid sequences of three human anaphylatoxins C3a, C4a, and C5a, using the program ClustalW.[77] A residue in bold indicates identity (also marked by the asterisks), and the colon (strongly similar) and single point (weakly similar) indicate homology. A dash (-) signifies a gap (i.e., insertion or deletion). The disulfide bridge patterns are shown at the top of the alignment and the α-helical segments (including fraying parts, see text) are shown for C3a and C5a.

elucidated using crystallographic and nuclear magnetic resonance (NMR) analyses, and will be the focus of the following paragraphs.

II. STRUCTURE OF C3a

The three-dimensional (3D) structures of human C3a and desArg-C3a were the first structures of a component of the complement system to be identified at atomic resolution (albeit at a relatively low resolution of about 3.2 Å). This work was done using x-ray crystallography by Huber et al., published in 1980.[34] Subsequently, one-dimensional NMR studies by Muto et al.[35,36] (for C3a, desArg-C3a, and C3a[1–69]), two-dimensional NMR studies by Nettesheim et al.[37] (for desArg-C3a) and Chazin et al.[38] (for C3a and desArg–C3a) determined the secondary structure of human C3a in solution. The latter also produced a very low-resolution tertiary structure of C3a.[39] The crystals of desArg-C3a and C3a produced identical diffraction patterns indicating that the two structures are very similar.[34] Similarity of the structures of human C3a and desArg-C3a was also indicated by NMR data[38] and at a coarser level by circular dichroism data.[33]

Figure 7.2A shows a ribbon model of the 3D crystal structure of human C3a.[34] This structure encompasses residues 13 (Gly) -77 (Arg). The missing amino-terminal residues did not produce diffraction patterns, resulting from either the presence of disorder or an ordered structure that is mobile in respect to the rest of the protein (a librational motion).[34] The latter is more likely since all solution NMR data identified the presence of a helix at this region. The crystal structure of C3a established the disulfide linkages between Cys22–Cys49, Cys23–Cys56, and Cys36–Cys57 (Figures 7.1 and 7.2A). The authors of this study described the structure of C3a as resembling a drumstick with very little internal core (Figure 7.2). The three cysteine bonds assist in the formation of the head piece and the long carboxy-terminal helix forms the stick protruding away from the head (Figure 7.2A). Our analysis using the program MolMol[40] with the implementation of the Kabsch and Sander algorithm for secondary structure identification[41] shows the presence of three α-helices. These are segments 17–23, 37–41, and 47–69. The NMR studies in combination[35–38] propose the presence of four α-helices in the residue segments 5–15 (with fraying in 5–7), 17–28 (with fraying in 17–18), 36–43, and 47–70 (with fraying in 67–70). The α-helices are connected with variable length loops and the amino- and carboxy-termini are in extended conformations. The NMR secondary structure identification was based on using combinations of (a) NOE connectivity patterns, (b) backbone spin–spin scalar coupling constants, (c) residue-specific hydrogen–deuterium exchange, and (d) qualitative line width analysis. Fraying at the helical termini is not unusual for α-helices in proteins, and it is observed by high hydrogen–deuterium exchange rates (or low protection factors) for backbone amide protons in exchange experiments and NMR spectroscopy (e.g., see Morikis[42]). Typically, the regular hydrogen-bonding pattern observed at the core of helices is weakened at the termini, thus contributing to high hydrogen–deuterium exchange rates and structural fraying (also described as transient or partial helix formation).

Figure 7.2B shows a stick model of the crystal structure of C3a that depicts the hydrophobic and charged character of C3a. The core of C3a is formed by the three

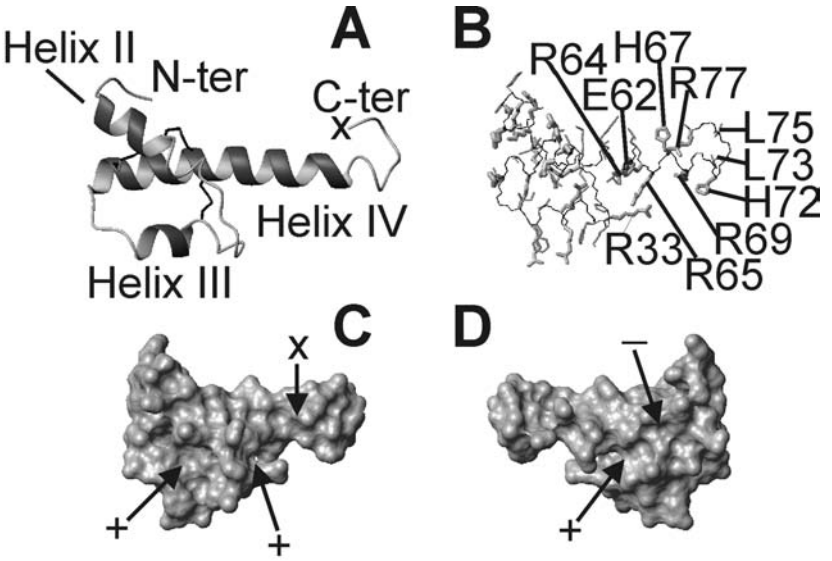

FIGURE 7.2 (A) Ribbon diagram of the structure of human C3a.[34] Only helices II–IV are present in the crystal structure (marked in figure). The disulfide bridges are shown and marked. (B) Stick representation of the backbone (in black thin lines) and hydrophobic and charged side chains (in grey thicker lines) of the structure of C3a. The remaining side chains are deleted for clarity. Side chains are drawn using lines of increased thickness in the following order: (a) hydrophobic side chains (Val, Leu, Ile, Thr, Phe, Tyr, Pro, Met) (there are no Trp residues in structure); (b) basic charged side chains (Arg, Lys, His); and (c) acidic charged side chains (Asp, Glu). Examples of a through c are shown with arrows. The orientation of the structure of C3a is the same as in panel A. (C) Molecular (contact) surface representation of human C3a to demonstrate the overall shape and the presence of cavities. The orientation of the structure of C3a is the same as in panel A. (D) Same as C but rotated by 180° around the vertical axis of the plane. Selected side chains that participate in the formation of structure and in binding, the binding site (x), and the charge character of cavities (+ for positive and – for negative) are marked in relevant panels. Molecular modeling was made using the program MolMol.[40] (Coordinates courtesy of R. Huber.)

disulfide bridges and to a lesser extent by interactions of hydrophobic side chains. The disulfide bridges hold together helices II and III, and the amino-terminus of helix IV. The NMR data suggest that helix I (missing in the crystal structure of Figure 7.2) packs between and behind helices II and IV (Figure 7.2A), but is mobile as a whole presumably because of lack of strong side-chain hydrophobic interactions. There is only one hydrophobic residue in the core of helix I (Val12), and one residue with hydrophobic character at the fraying region (Thr5). There is no evidence of aromatic packing interactions in Figure 7.2B. There is an excess of positive charge in C3a (Figure 7.2B; color Figure 7.2B through F on companion CD). Salt bridges that contribute to local and packing interactions of C3a are observed for the pairs Glu24–Arg20, Asp25–Arg28, Glu62–Arg65, and weaker salt bridges are observed for the pairs Asp25–Arg39, Asp55–Lys51, Glu24–Lys17, Glu47–Lys50. It is not clear what the role is of the two carboxy-terminal histidines, His67 and His72.

Figure 7.2C and D show two views of the surface of C3a that depict the presence of cavities. The proposed interaction site with C3aR is marked with an arrow. These are C3a carboxy-terminal residues 69–77, which have a predominantly positively charged character (Figure 7.2B). The current binding model of C3a to its receptor C3aR involves interaction of this carboxy-terminal tail (marked in Figure 7.4C) with an unusually long extracellular loop connecting helices IV and V of the seven-helix transmembrane C3aR receptor (Figure 7.4).[43] These interactions are presumably electrostatic. Three out of four cavities in Figure 7.2C and D are also positively charged while the fourth cavity is negatively charged (color Figure 7.2C through F on companion CD). It is not known if these cavities have binding and physiological function.

A. Differences between the Crystal and Solution Structures at C3a Amino Terminal Region

Two major differences were observed in the secondary structures from the crystal and solution phase studies. First, the NMR data identified an additional amino-terminal helix,[37,38] which did not produce visible electron density in the crystalline form (missing in Figure 7.2).[34] Second, the NMR data demonstrated the presence of dynamic extended conformation at the carboxy-terminus beyond residue 66,[37,38] while the crystallographic data showed the presence of helical conformation until residue 73 (out of a total 77 residues), with the remaining four residues being at an extended but stable conformation.[34] This difference was attributed to the interaction of two molecules in the crystal with helix IV arranged in antiparallel fashion.[34,37] The same interaction could explain the observed stable conformation of the remaining four terminal residues in the crystal. Less significant differences are seen in the beginning and ending of the other two helices, but this is not unusual when comparing crystallographic and NMR data (e.g., Morikis et al.[44]). In consensus, by putting together the NMR and crystallographic data, C3a forms a four-helix bundle in agreement with the structural motif of the core of C5a. We have named the four α-helices I–IV, with I being the amino-terminal helix (seen only in NMR data), and IV being the carboxy-terminal helix. We will use the same notation for C5a (see below) to facilitate the comparison with C3a.

We should note here that the structure of C3a was of lower resolution resulting from small crystal size and about 30% contamination with desArg-C3a; however, the authors had evidence that the crystallized form belongs to C3a.[34]

B. Stability of C3a

The NMR studies were conducted at several pH values spanning a pH range of 2.3 to 7.5, and at several temperatures spanning the range between 10°C to 35°C. In the crystallographic studies, crystals were grown at pH 4.5. C3a and desArg-C3a are stable in these pH and temperature ranges as indicated by the consistency of the NMR data and the determined secondary structure. This is also supported by circular dichroism data.[33] Denaturation studies using reducing agents also showed that the structure of C3a is very stable and is capable of reversible denaturation.[33]

C. Activity of C3a

C3a is a protein of 77 residues, of which the carboxy-terminal Arg77 is essential for activity. Despite the general loss of activity upon removal of Arg77, the structures of C3a and desArg-C3a are nearly identical.[34,38] It is not clear whether the core of the structure of C3a formed by helices I–III simply serves as a stabilizer of helix IV (the carboxy-terminal helix) or has a functional role by binding to a receptor.[34] A synthetic peptide derived from the sequence of the 21 carboxy-terminal residues has shown 50% to 100% activity compared to native C3a;[45] however, synthetic peptides of the 13 and 8 carboxy-terminal residues showed only 4% to 8% and 2% to 3% activity, respectively, and terminal penta- and tetrapeptides showed negligible activity.[45] It should be noted that the carboxy-terminal pentapeptide Leu-Gly-Leu-Ala-Arg is conserved among various species, as are the three pairs of disulfide bridges. The observed differences between the NMR and crystal secondary structures in the carboxy-terminal region should be critically examined when structure–function relations are used to study binding properties or to design inhibitory sequences.

III. STRUCTURE OF C5a

The 3D structure of recombinant human C5a was determined using NMR by the Zuiderweg[46] and Zhang[47] groups. The structure by Zuiderweg et al.[46] was well defined for residues 1 to 63 (out of a total 74), and undefined for the carboxy-terminal residues 64 to 74, which showed dynamic random-coil conformation. However, the structure by Zhang et al.[47] showed α-helical conformation in the region 69–74. The remaining regions are consistent in the structures determined by Zuiderweg et al.[46] and Zhang et al.[47]

The 3D structure of porcine desArg-C5a (with cleaved carboxy-terminal Arg74) was determined using NMR by Williamson et al.[48] Also, the secondary structure of bovine C5a(5–66) was determined using NMR by Zarbock et al.[49] Both of these structures showed a random configuration at the carboxy-terminus, in agreement with the structure of recombinant human C5a by Zuiderweg et al.,[46] and in disagreement with the structure of recombinant human C5a by Zhang et al.[47]

Figure 7.3A shows a ribbon model of a representative 3D solution structure of recombinant human C5a out of a total 20 structures in the NMR ensemble.[47] This structure encompasses residues 1 (Met) -74 (Arg) (Thr1 was replaced by Met1 by the bacterial expression system). C5a has disulfide linkages between Cys21–Cys47, Cys22–Cys54, and Cys34–Cys55. A fifth free cysteine, Cys27, is located at the end of helix II. The structural motif of C5a is a four-helix bundle of helices running in an antiparallel fashion to each other, with an additional fifth helix at the carboxy-terminus. The four-helix bundle segment is of the unicornate type according to the definition of Harris et al.[50] Unicornate-type four-helix bundles have the topology of parallel-parallel-orthogonal-orthogonal arrangement for four consecutive helix pairs (helix pairs 4-1, 1-2, 2-3, 3-4 for C5a; analysis made using the program MolMol[40]). A secondary structure analysis of recombinant human C5a[47] using the implementation of the Kabsch and Sander algorithm[41] within the program MolMol[40] shows five α-helices comprising residue segments 5–11 (helix I), 16–27 (II), 34–38 (III),

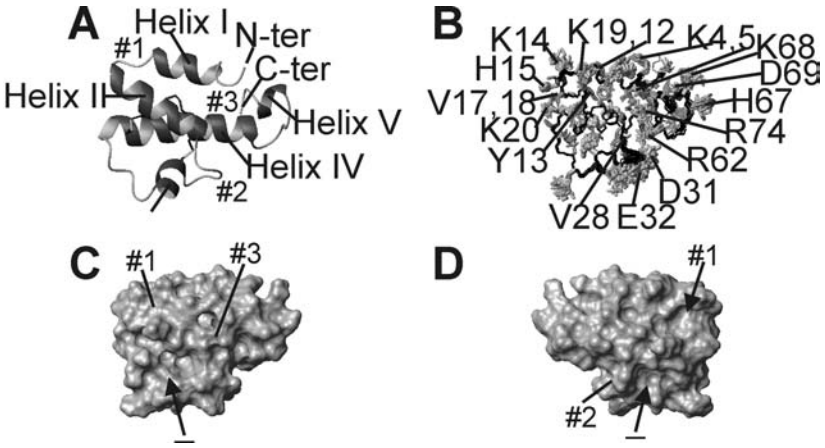

FIGURE 7.3 (A) Ribbon diagram for a representative NMR structure of recombinant human C5a.[47] The disulfide bridges and free Cys27 are shown and marked. (B) Stick representation of the backbone (in black thin lines) and hydrophobic and charged side chains (in grey thicker lines) of the ensemble of 20 low-energy structures of C5a. The remaining side chains are deleted for clarity. Side chains are drawn using lines of increased thickness in the following order: (a) hydrophobic side chains (Val, Leu, Ile, Thr, Phe, Tyr, Pro, Met) (there are no Trp residues in structure); (b) basic charged side chains (Arg, Lys, His); and (c) acidic charged side chains (Asp, Glu). Examples of a through c are shown with arrows. The orientation of the structure of C5a is the same as in panel A. (C) Molecular (contact) surface representation for a representative structure of recombinant human C5a to demonstrate the overall shape and the presence of cavities. The orientation of the structure of C5a is the same as in panel A. (D) Same as C but rotated by 180° around the vertical axis of the plane. Selected side chains that participate in the formation of structure and in binding, the binding sites #1, #2, #3, and the charge character of cavities (+ for positive and – for negative) are marked in relevant panels. Molecular modeling was made using the program MolMol.[40] (Coordinates from NMR structure with PDB code 1KJS.)

45–62 (IV), and 68–71 (V). The NMR studies in combination[46,47] propose the presence of five α-helices in the residue segments 4–13 (with fraying at 4 and 12–13), 16–28 (with fraying in 16–19, 28), 33–39 (with fraying at 33, 39), 45–64 (with fraying at 45, 63–64), and 68–74 (with fraying at 68, 72–74). The α-helices are connected with variable length loops. Helices I to IV form the core of C5a, and the carboxy-terminal region, including helix V, forms a small tail.

Figure 7.3B shows a stick model of the ensemble of NMR structures of recombinant human C5a[47] that depicts the hydrophobic and charged character of C5a. As in the case of C3a, the core of C5a is formed by the three disulfide bridges, and to a lesser extent by interactions of hydrophobic side chains. The disulfide bridges hold together helices II, III, and IV. Helix I is packed against the rest mainly through hydrophobic interaction involving Ile6 and Ile9. As in the case of C3a, there is no evidence of aromatic packing interactions (Figure 7.3B). There is an excess of positive charge in C5a (Figure 7.3B); however, the negative charge is more localized within two major (in size) cavities located at opposite surfaces to each other and a

minor cavity (color Figure 7.3B through F on companion CD). A salt bridge that contributes to a local interaction is observed for the pair Glu8–Lys4, and weaker salt bridges that contribute to either local or packing interactions are observed for the pairs Asp24–Lys20, Asp31–Arg62, Glu7–Lys4, Glu7–Lys19, Glu8–Lys4, Glu8–Lys5, Glu8–Lys12, Glu35–Lys20, Glu53–Lys5, Glu53–Lys12, Glu53–Lys49. Figure 7.3B shows that the side chains of Arg62 and Arg74 are positioned in relative proximity (to within 4.6 to 8.3 Å for the Cζ atom of their guanadinium groups in the ensemble of 20 NMR structures of Zhang et al.[47] The lone Cys27 is located within 3.7-6.6 Å from carboxy-terminal Arg74 (using the distance between Cys27 Sγ-Arg74 Cζ in the ensemble of 20 NMR structures of Zhang et al.[47] This is a favorable interaction that possibly stabilizes the local structure. The role of the two histidines, His15 and His67, may be to modulate local charge distribution depending on their local (apparent) pK_a (for instance, see Morikis et al.[51,52] for a discussion on the role of His apparent pK_as) and the solution pH.

Figure 7.3C and D shows two views of the surface of C5a that depict the presence of cavities. A major cavity is observed in the view of Figure 7.3C and a major and a minor cavity are observed in the view of Figure 7.3D. The major cavities have acidic character and the minor cavity has basic character (color Figure 7.3E and F on companion CD). Proposed interaction sites of C5a with its seven-helix transmembrane receptor C5aR (Figure 7.4) include three sequentially discontinuous regions of C5a (marked in Figure 7.3C and D). These involve: (a) the loop between helices I and II of C5a interacting with the amino-terminal extracellular extended domain and the extracellular loop connecting helices IV and V (close to helix V, known as the "recognition site") of C5aR;[53–57] (b) the loop between helices III and IV of C5a interacting with the extracellular loop between helices IV and V of C5aR;[53,54] and (c) the carboxy-terminal region of C5a interacting with the (upper third of the) fifth transmembrane helix (called the "effector site") of C5aR.[53–55,57–60] These interactions are presumably electrostatic, involving negative charges in the amino-terminal extracellular domain of C5aR, and positive and negative charges of the carboxy-terminal Arg of C5a (positive for side chain and negative for backbone at pH ~3.8 and above). The C5a site of interaction between helices I and II forms the minor cavity of basic character (see above) (Figure 7.3 and color Figure 7.3 on companion CD). The other two sites of interaction do not form cavities. Rather than trying to match individual residues of opposite charge in the sequences of C5a and C5aR in the absence of a 3D structure of C5aR, it may be worth speculating that all charged cavities on the surface of the four-helix bundle of C5a (Figure 7.3C and D; color Figure 7.3C through F on companion CD) may interact with the recognition site of C5aR in a way that is not yet identified. Conformational changes upon binding are also expected to alter side-chain orientations and molecular surfaces.

A. C5a Structures from Different Species

Similar to C3a, the carboxy-terminal part of C5a is relatively conserved among species, and generally consists of the effector sequence (Met/Ile/Val)-Gln-Leu-Gly-Arg. Structural similarities can also be observed at other levels, as the secondary structures and the overall folds of recombinant human C5a,[46,47] bovine C5a(5–66),[49]

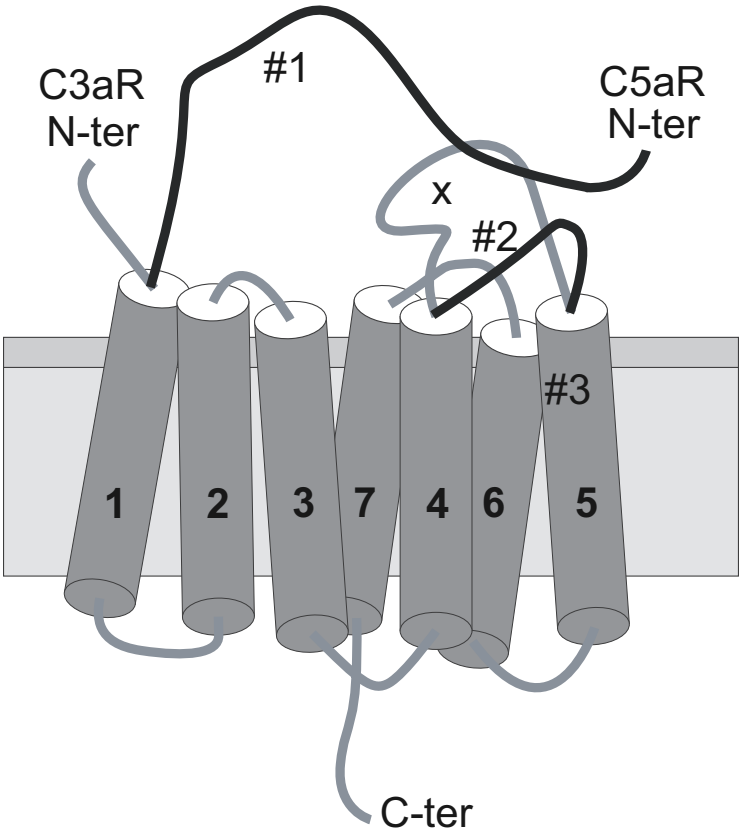

FIGURE 7.4 Cartoon model of C3aR and C5aR. The C3aR and C5aR receptors are G-protein coupled rhodopsin-like transmembrane proteins, comprising seven transmembrane helices, connecting extra- and intracellular loops of variable length, an extracellular amino-terminal extended domain, and an intracellular extended carboxy-terminal domain. Currently, there are no 3D structures of C3aR or C5aR. The cartoon of this figure is based on a rhodopsin structure from the Protein Data Bank, but is not drawn in scale. C5aR has a longer amino-terminal domain and a shorter extracellular loop connecting helices IV to V (in black) than C3aR (in grey). The approximate sites of proposed interaction with C3a (x) and C5a (#1, #2, #3) are marked.

and porcine desAr74-C5a[48] are very similar for helices I to IV, with some differences in the interhelical loop segments. Only the structure of recombinant human C5a[47] demonstrated a clear fifth helix (helix V) at the carboxy-terminus (Figure 7.3).

The coordinates of the structures of recombinant human C5a (residues 1 to 74)[47] and porcine desArg77-C5a (residues 1 to 65)[48] are available from the Protein Data Bank[61] and have codes 1KJS and 1C5A, respectively.

B. Differences in NMR Structures of Carboxy-Terminal Region of C5a

The origin of the discrepancy on the definition of the structure (or lack of) in the region of residues 69 to 74 is not clear in the studies of Zuiderweg et al.[46] and Zhang et al.[47] The 3D structure of Zhang et al.[47] was determined at pH 5.2 and 30°C, while the structure of Zuiderweg et al.[46] was determined at pH 2.3 and 10°C. However, Zuiderweg et al.[46] collected additional NMR data at pH values of 2.3 and 5.5 for recombinant C5a and pH 2.3 for recombinant C5a without Met1, and pH 6.0 at 20°C, none of which indicated structure at the carboxy-terminus. Zuiderweg et al.[46] concluded that the lack of structure beyond residue 63 was not a pH artifact or recombination artifact due to the presence of Met1. Another significant observation of Zuiderweg et al.[46] was that the NMR data for the region 64–70 did not support a complete random coil conformation but a dynamic ensemble with some helical characteristics, with the remaining four carboxy-terminal residues being at complete disorder. This observation was based on nuclear Overhauser effect (NOE) connectivity patterns, hydrogen–deuterium exchange of amide protons, chemical shift values, and line width values. However, Zhang et al.[47] proposed that lowering the pH from 5.2 to 2.3 resulted in random coil conformation in the 69–74 region. This observation was based on chemical shift values and hydrogen–deuterium exchange of amide protons, using ^{1}H-^{15}N heteronuclear NMR data. In our opinion, another factor contributing to the discrepancy in the structure definition of the carboxy-terminal hexapeptide of C5a may be technical owed to the higher resolution of heteronuclear ^{1}H and ^{15}N NMR (in addition to the homonuclear ^{1}H data) of Zhang et al.[47] using isotopically labeled C5a, as opposed to the homonuclear ^{1}H NMR data of Zuiderweg et al.[46] Indeed, Zuiderweg et al.[46] discussed spectral overlap in the region beyond residue 65 that contributes to low spectral resolution. Another contributing factor in the discrepancy may be the different NOE mixing times used by the two studies, up to 200 ms in Zhang et al.[47] as opposed to up to 100 ms in Zuiderweg et al.[46]

C. Stability of C5a

The structure of recombinant human C5a is stable at the pH range 2.3 to 6.0 and at temperatures 10°C to 30°C, with the exception of the carboxy-terminal hexapeptide comprising residues Asp69-Met-Gln-Leu-Gly-Arg74 (see above for a discussion on discrepancies between the two NMR structures). The latest NMR studies show a well-defined α-helix in this segment at pH 5.2, which unravels to a random coil conformation at pH 2.3.[47]

D. Activity of C5a

Cleavage of Arg74 by carboxypeptidases generates the less potent desArg-C5a fragment. Despite the activity- and species-related differences, the overall folds of recombinant human C5a[62] and porcine desArg-C5a[48] are very similar. However, we

should bear in mind that the two recombinant human C5a structures[47,62] show a potentially functionally significant difference in the carboxy-terminal region.

The binding of C5a to its receptor C5aR is a two-step process with three sites in C5a and three sites on C5aR[54–57,63,64] known thus far. The first step involves the four-helix bundle portion of C5a and the recognition site of C5aR. The second step involves the carboxy-terminal tail with the fifth helix of C5a and the effector site of C5aR. Conformational changes have also been proposed to accommodate binding.[53,56,58] This binding model has been proposed to act as a molecular switch activated by C5a that transmits extracellular signal from C5a to intracellular G protein.[55]

As discussed above, early mutagenesis studies have shown that carboxy-terminal residues Arg74 and Lys68 are responsible for interactions with C5aR.[53] Several subsequent studies of small peptides derived from the sequence of the carboxy-terminal region of C5a and from sequence improvements have shown agonist activities.[65–68]

The carboxy-terminal tail of C5a has been used as a template to design low-molecular-mass antagonists for receptor binding. C5a plays an important role in inflammation (see above), and therefore, this complement protein makes a good target for the development of anti-inflammatory drugs. Currently, there are no drugs in the clinic that target complement, but the availability of such compounds would be beneficial in various pathological situations where external complement regulation is needed[69] (see above). Several timely efforts have focused on the development of C5a antagonists, based on sequence modifications of the carboxy-terminal region of C5a (reviewed in Morikis and Lambris[70]). Most of the early efforts resulted in the identification of agonists and recent efforts, most by Stephen Taylor and coworkers, have resulted in the identification of antagonists.[29,67,71–73] In Chapter 15, Taylor and Fairlie review the most active C5aR antagonist peptide.[74]

In another study, Zhang et al.[75] designed a semisynthetic C5aR antagonist using a modified version of C5a, structure 1CFA of the Protein Data Bank.[61] They combined recombinant human C5a(1–71), with replacements Thr1Met, Cys27Ser, Gln71Cys, and a synthetic peptide with sequence Cys72-Leu-Gly-DArg75. The connection of the two constructs was made through a disulfide bridge between Cys71 and Cys72. The rationale behind this construct was to position the carboxy-terminal D-Arg (here D-Arg75) in proximity to Arg46 and His15, thus enhancing a positively charged surface by DArg75/Arg46/Lys49/His15. The underlying assumption was that a single C5aR-binding site (the negatively charged extracellular region) was responsible for antagonist activity.[75] The authors of this study also point out that a single C5aR-binding site is not sufficient for agonist activity. Other C5a-like antagonists with modified carboxy-terminal tails have also been reported.[76]

IV. COMPARISON OF HUMAN C3a AND C5a STRUCTURES

Figure 7.5 shows a superimposition of the 3D structures of human C3a[34] and recombinant human C5a.[47] Both structures form four-helix bundles (helices I–IV), but C5a contains an additional fifth helix at the carboxy-terminus, which extends away from

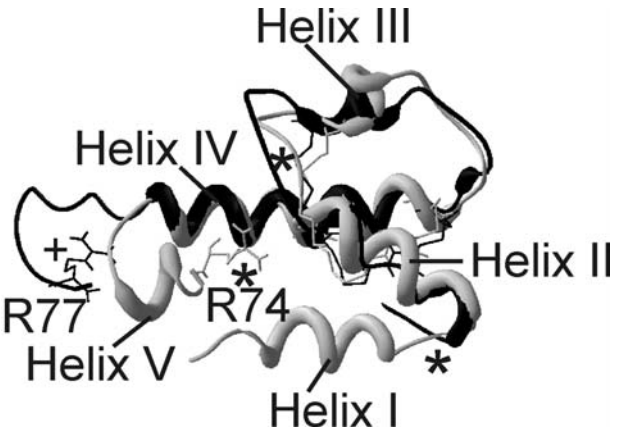

FIGURE 7.5 Comparison of structures of C3a and C5a. The crystal structure of C3a[34] (in black) and a representative solution structure of C5a[47] (in grey) have been superimposed using the backbone Cα atoms. The cysteines and carboxy-terminal arginines are also shown. (C3a coordinates courtesy of R. Huber; C5a coordinates from NMR structure with PDB code 1KJS.)

the bundle. In Figure 7.5, helix I of the crystal structure of C3a is missing. Although the structure of C5a can be classified as a four-helix bundle of the unicornate type with an additional hanging fifth helix, a similar classification is not possible for C3a because of the missing first helix. However, a unicornate type is not possible for C3a because of the difference in position of helix III, which is parallel to helix IV in C3a as opposed to being orthogonal in C5a (Figure 7.5).

V. CONCLUDING REMARKS

The anaphylatoxins are remarkable proteins with respect to their high resistance to denaturation and ability to spontaneously refold to their native structure upon removal of the denaturing conditions. These characteristics result from the presence of three pairs of disulfide bridges and the high level of helicity, which contribute to the formation of stable protein cores. Although the carboxy-terminal part of these compounds contains an important effector site, other regions of the C3a and C5a molecules have been shown to be involved in mediating the binding of C3a and C5a to their respective receptors. Studies carried out using various truncated and mutated molecules, as well as the determination of the three dimensional structures of C3a and C5a, have provided important information on the structural–functional relationships of these compounds. Consequently, various selective C3aR and C5aR agonists and antagonists have been developed that show promise for a wide range of research and clinical applications. Although C4a has not been scrutinized in a manner similar to C3a and C5a, we expect that this line of research will intensify in the near future. Finally, we expect that new and potent antagonists for receptor binding will be designed for C3a and C4a in a similar fashion as has been done for C5a.

ACKNOWLEDGMENTS

This work was supported by grants from the National Institutes of Health and the American Heart Association. We thank Robert Huber for providing the crystallographic coordinates of C3a structure.

SUPPLEMENTARY MATERIAL ON CD

All figures, including Figures 7.2, 7.3, and 7.5 in color, and their corresponding figure captions are supplied on the companion CD.

The coordinates of the crystal structure of human C3a are included on the companion CD (with permission; code C3a_HUBER, not deposited with the Protein Data Bank).

REFERENCES

1. M Huber-Lang, EM Younkin, JV Sarma, N Riedemann, SR McGuire, KT Lu, R Kunkel, JG Younger, FS Zetoune, PA Ward. *Am. J. Pathol.*, 161:1849–1859, 2002.
2. E Friedberger. Weitere Untersuchungen uber Eisissanaphylaxie: IV. *Mitteilung Immunitaetaforsch Exp. Ther.*, 4:636–690, 1910.
3. JA Ember, MA Jagels, TE Hugli. In JE Volanakis, MM Frank, Eds. *The Human Complement System in Health and Disease*. Marcel Dekker, New York, 1998, pp. 241–284.
4. RA Wetsel, J Kildsgaard, DL Haviland. In JD Lambris, MV Holers, Eds. *Therapeutic Interventions in the Complement System*. Humana Press, Totowa, NJ, 2000, pp. 113–153.
5. SA Cain, PN Monk. *J. Biol. Chem.*, 277:7165–7169, 2002.
6. S Okinaga, D Slattery, A Humbles, Z Zsengeller, O Morteau, MB Kinrade, RM Brodbeck, JE Krause, HR Choe, NP Gerard, C Gerard. *Biochemistry*, 42:9406–9415, 2003.
7. D Mastellos, J Lambris. *Trends Immunol.*, 23:485, 2002.
8. CW Strey, M Markiewski, D Mastellos, R Tudoran, LA Spruce, LE Greenbaum, JD Lambris. *J. Exp. Med.*, 198:913–923, 2003.
9. R Reca, D Mastellos, M Majka, L Marquez, J Ratajczak, S Franchini, A Glodek, M Honczarenko, LA Spruce, A Janowska-Wieczorek, JD Lambris, MZ Ratajczak. *Blood*, 101:3784–3793, 2003.
10. I Farkas, L Baranyi, M Takahashi, A Fukuda, Z Liposits, T Yamamoto, H Okada. *J. Physiol. (London),* 507:679–687, 1998.
11. J van Beek, O Nicole, C Ali, A Ischenko, ET MacKenzie, A Buisson, M Fontaine. *Neuroreport*, 12:289–293, 2001.
12. G Girardi, J Berman, P Redecha, L Spruce, JM Thurman, D Kraus, TJ Hollman, P Casali, MC Caroll, RA Wetsel, JD Lambris, VM Holers, JE Salmon. *J. Clin. Invest.*, 112:1644–1654, 2003.
13. W Campbell, N Okada, H Okada. *Immunol. Rev.*, 180:162–167, 2001.
14. I Murray, J Kohl, K Cianflone. *Biochem. J.*, 342:41–48, 1999.

15. I Murray, RA Parker, TG Kirchgessner, J Tran, ZJ Zhang, J Westerlund, K Cianflone. *J. Lipid Res*., 38:2492–2501, 1997.
16. P Langkabel, J Zwirner, M Oppermann. *Eur. J. Immunol*., 29:3035–3046, 1999.
17. N Naik, E Giannini, L Brouchon, F Boulay. *J. Cell Sci*., 110:2381–2390, 1997.
18. DE Hammerschmidt, LJ Weaver, LD Hudson, PR Craddock, HS Jacob. *Lancet*, 1:947–949, 1980.
19. AA Humbles, B Lu, CA Nilsson, C Lilly, E Israel, Y Fujiwara, NP Gerard, C Gerard. *Nature*, 406:998–1001, 2000.
20. BJ Czermak, V Sarma, CL Pierson, RL Warner, M Huber-Lang, NM Bless, H Schmal, HP Friedl, PA Ward. *Nat. Med*., 5:788–792, 1999.
21. G Moxley, S Ruddy. *Arthritis Rheum*., 28:1089–1095, 1985.
22. TM Woodruff, AJ Strachan, N Dryburgh, IA Shiels, RC Reid, DP Fairlie, SM Taylor. *Arthritis Rheum*., 46:2476–2485, 2002.
23. O Ahrenstedt, L Knutson, B Nilsson, K Nilsson-Ekdahl, B Odlind, R Hallgren. *N. Engl. J. Med*., 322:1345–1349, 1990.
24. P Mukherjee, GM Pasinetti. *J. Neuroimmunol*., 105:124–130, 2000.
25. U Mrowietz, WA Koch, K Zhu, O Wiedow, J Bartels, E Christophers, JM Schroder. *Exp. Dermatol*., 10:238–245, 2001.
26. RY Chen, G Ning, ML Zhao, MG Fleming, LA Diaz, Z Werb, Z Liu. *J. Clin. Invest*., 108:1151–1158, 2001.
27. RS Ames, D Lee, JJ Foley, AJ Jurewicz, MA Tornetta, W Bautsch, B Settmacher, A Klos, KF Erhard, RD Cousins, AC Sulpizio, JP Hieble, G McCafferty, KW Ward, JL Adams, WE Bondinell, DC Underwood, RR Osborn, AM Badger, HM Sarau. *J. Immunol*., 166:6341–6348, 2001.
28. TV Arumugam, IA Shiels, AJ Strachan, G Abbenante, DP Fairlie, SM Taylor. *Kidney Int*., 63:134–142, 2003.
29. DR Haynes, DG Harkin, LP Bignold, MJ Hutchens, SM Taylor, DP Fairlie. *Biochem. Pharmacol*., 60:729–733, 2000.
30. T Heller, M Hennecke, U Baumann, JE Gessner, AM zu Vilsendorf, M Baensch, F Boulay, A Kola, A Klos, W Bautsch, J Kohl. *J. Immunol*., 163:985–994, 1999.
31. A Short, AK Wong, AM Finch, G Haaima, IA Shiels, DP Fairlie, SM Taylor. *Br. J. Pharmacol*., 126:551–554, 1999.
32. C Gerard, DE Chenoweth, TE Hugli. *J. Immunol*., 127:1978–1982, 1981.
33. TE Hugli, WT Morgan, HJ Müller-Eberhard. *J. Biol. Chem*., 250:1479–1483, 1975.
34. R Huber, H Scholze, EP Paques, J Deisenhofer. *Hoppe-Seylers Z Physiol Chem*., 361:1389–1399, 1980.
35. Y Muto, Y Fukumoto, Y Arata. *J. Biochem*., 102:635–641, 1987.
36. Y Muto, Y Fukumoto, Y Arata. *Biochemistry*, 24:6659–6665, 1985.
37. DG Nettesheim, RP Edalji, KW Mollison, J Greer, ERP Zuiderweg. *Proc. Natl. Acad. Sci. U.S.A*., 85:5036–5040, 1988.
38. WJ Chazin, TE Hugli, PE Wright. *Biochemistry*, 27:9139–9148, 1988.
39. MW Kalnik, WJ Chazin, PE Wright. In JJ Villafranca, Ed. *Techniques in Protein Chemistry II*. Academic Press, San Diego, 1991, pp. 393–400.
40. R Koradi, M Billeter, K Wuthrich. *J. Mol. Graph*., 14:51–55, 1996.
41. W Kabsch, C Sander. *Biopolymers*, 22:2577–2637, 1983.
42. D Morikis, PE Wright. *Eur. J. Biochem*., 237:212–220, 1996.
43. TH Chao, JA Ember, MY Wang, Y Bayon, TE Hugli, RD Ye. *J. Biol. Chem*., 274:9721–9728, 1999.
44. D Morikis, CA Lepre, PE Wright. *Eur. J. Biochem*., 219:611–626, 1994.

45. TE Hugli. In JD Lambris, Ed. *The Third Component of Complement*. Springer-Verlag, Heidelberg, 1989, pp. 181–208.
46. ERP Zuiderweg, DG Nettesheim, KW Mollison, GW Carter. *Biochemistry*, 28:172–185, 1989.
47. XL Zhang, W Boyar, MJ Toth, L Wennogle, NC Gonnella. *Proteins*, 28:261–267, 1997.
48. MP Williamson, VS Madison. *Biochemistry*, 29:2895–2905, 1990.
49. J Zarbock, R Gennaro, D Romeo, GM Clore, AM Gronenborn. *FEBS Lett.*, 238:289–294, 1988.
50. NL Harris, SR Presnell, FE Cohen. *J. Mol. Biol.*, 236:1356–1368, 1994.
51. D Morikis, AH Elcock, PA Jennings, JA McCammon. *Protein Sci.*, 10:2363–2378, 2001.
52. D Morikis, AH Elcock, PA Jennings, JA McCammon. *Protein Sci.*, 10:2379–2392, 2001.
53. KW Mollison, W Mandecki, ER Zuiderweg, L Fayer, TA Fey, RA Krause, RG Conway, L Miller, RP Edalji, MA Shallcross. *Proc. Natl. Acad. Sci. U.S.A.*, 86:292–296, 1989.
54. MS Huber-Lang, JV Sarma, SR McGuire, KT Lu, VA Padgaonkar, EM Younkin, RF Guo, CH Weber, ER Zuiderweg, FS Zetoune, PA Ward. *J. Immunol.*, 170:6115–6124, 2003.
55. JA Demartino, G Vanriper, SJ Siciliano, CJ Molineaux, ZD Konteatis, H Rosen, MS Springer. *J. Biol. Chem.*, 269:14446–14450, 1994.
56. ZG Chen, XL Zhang, NC Gonnella, TC Pellas, WC Boyar, F Ni. *J. Biol. Chem.*, 273:10411–10419, 1998.
57. SJ Siciliano, TE Rollins, J DeMartino, Z Konteatis, L Malkowitz, G Van Riper, S Bondy, H Rosen, MS Springer. *Proc. Natl. Acad. Sci. U.S.A.*, 91:1214–1218, 1994.
58. JA Demartino, ZD Konteatis, SJ Siciliano, G Vanriper, DJ Underwood, PA Fischer, MS Springer. *J. Biol. Chem.*, 270:15966–15969, 1995.
59. U Raffetseder, D Roper, L Mery, C Gietz, A Klos, J Grotzinger, A Wollmer, F Boulay, J Kohl, W Bautsch. *Eur. J. Biochem.*, 235:82–90, 1996.
60. J Grotzinger, M Engels, E Jacoby, A Wollmer, W Strassburger. *Protein Eng.*, 4:767–771, 1991.
61. HM Berman, J Westbrook, Z Feng, G Gilliland, TN Bhat, H Weissig, IN Shindyalov, PE Bourne. *Nucleic Acids Res.*, 28:235–242, 2000.
62. ERP Zuiderweg, KW Mollison, J Henkin, GW Carter. *Biochemistry*, 27:3568–3580, 1988.
63. DE Chenoweth, TE Hugli. *Mol. Immunol.*, 17:151–161, 1980.
64. L Mery, F Boulay. *J. Biol. Chem.*, 269:3457–3463, 1994.
65. JA Ember, SD Sanderson, SM Taylor, M Kawahara, TE Hugli. *J. Immunol.*, 148:3165–3173, 1992.
66. M Kawai, DA Quincy, B Lane, KW Mollison, JR Luly, GW Carter. *J. Med. Chem.*, 34:2068–2071, 1991.
67. ZD Konteatis, SJ Siciliano, G Vanriper, CJ Molineaux, S Pandya, P Fischer, H Rosen, RA Mumford, MS Springer. *J. Immunol.*, 153:4200–4205, 1994.
68. M Kawai, DA Quincy, B Lane, KW Mollison, YS Or, JR Luly, GW Carter. *J. Med. Chem.*, 35:220–223, 1992.

69. JD Lambris, VM Holers. *Therapeutic Interventions in the Complement System*. Humana Press, Totowa, NJ, 2000.
70. D Morikis, JD Lambris. *Biochem. Soc. Trans.*, 30, 1026–1036, 2002.
71. AK Wong, AM Finch, GK Pierens, DJ Craik, SM Taylor, DP Fairlie. *J. Med. Chem.*, 41:3417–3425, 1998.
72. AM Finch, AK Wong, NJ Paczkowski, SK Wadi, DJ Craik, DP Fairlie, SM Taylor. *J. Med. Chem.*, 42:1965–1974, 1999.
73. BO Gerber, EC Meng, V Dotsch, TJ Baranski, HR Bourne. *J. Biol. Chem.*, 276:3394–3400, 2001.
74. SM Taylor, D Fairlie. In D Morikis, JD Lambris, Eds. *Structural Biology of the Complement System*. Marcel Dekker, New York, 2005.
75. XL Zhang, W Boyar, N Galakatos, NC Gonnella. *Protein Sci.*, 6:65–72, 1997.
76. TC Pellas, W Boyar, J van Oostrum, J Wasvary, LR Fryer, G Pastor, M Sills, A Braunwalder, DR Yarwood, R Kramer, E Kimble, J Hadala, W Haston, R Moreira-Ludewig, S Uziel-Fusi, P Peters, K Bill, LP Wennogle. *J. Immunol.*, 160:5616–5621, 1998.
77. J Thompson, D Higgins, T Gibson. *Nucleic Acids Res.*, 22:4673, 1994.